ULTRASONIC CHARACTERIZATION OF DEFECT ROOT GEOMETRY

A.N. Sinclair and H. Wang
Department of Mechanical Engineering
University of Toronto
Toronto, Ontario Canada M5S-1A4

D. Mair, M.D.C. Moles, and M. Dolbey
Ontario Hydro Technologies
800 Kipling Avenue
Toronto, Ontario Canada M8Z-5S4

BACKGROUND

The potential for crack initiation at a surface-breaking defect is strongly dependent on the radius of curvature ρ at the defect root: a small radius can lead to large stress concentrations which greatly increase the risk of crack initiation. In this project, the objective is to develop a technique for estimating the radius of curvature at the root of a fretting wear defect on the inside surface of a CANDU nuclear reactor pressure tube.

One unusual aspect to this problem is that many geometrical features of the defects under investigation are already known. The defects are in the shape of flat-bottomed axial gouges approximately 3 mm wide. Their depths, which range up to a few hundred microns, can be accurately estimated by ultrasonic time-of-flight techniques. [1] The radius of curvature at the bottom corners of the gouge is the only significant feature for which no information is readily obtainable by any conventional nondestructive technique in the hostile environment of a nuclear reactor core.

WAVE THEORY

Considerable work has been done on the diffraction of ultrasound from geometric discontinuities. Characterization of surface-breaking defects such as those under investigation here has frequently been conducted using Rayleigh waves. Features such as defect depth and surface roughness have been studied, e.g. [2,3], but generally for defects that were very sharp cracks or had idealized shapes such as hemispherical pits. [4] The

Review of Progress in Quantitative Nondestructive Evaluation, Vol. 14
Edited by D.O. Thompson and D.E. Chimenti, Plenum Press, New York, 1995

significant influence of the root radius of curvature on such work has been noted, but not pursued [5].

The possibility of estimating ρ using bulk waves holds more promise, as results would not be corrupted by variable surface roughness of the component as in the case of Rayleigh waves. From a qualitative standpoint, the dependence of the ultrasonic diffraction pattern on ρ/λ, where λ is the ultrasound wavelength, is well known: values of ρ/λ that are much less than 1 lead to an isotropic diffraction pattern, while values much greater than 1 are characterized by specular reflection.

The complicated shape of a fret mark inhibits the use of analytical techniques to obtain a precise description of the diffraction pattern of a wave incident on these defects. Although numerical techniques such as finite difference, finite element, or boundary element methods could be used to predict the diffraction pattern as a function of incident angle, diffraction angle, and ρ/λ, such techniques are expensive and fail to account for many of the experimental difficulties that complicate nondestructive evaluation.

To address this problem, the wave diffraction pattern from a 270-degree corner of finite radius will be studied using a new type of immersion reference block. Shear waves are chosen in order to bring the wavelength to the same general magnitude as that expected for the radius of curvature (50 - 400 microns). The mode conversion process used to generate the shear waves in both pressure tube inspection and the reference block results in a vertical polarization (SV).

EXPERIMENT

Reference Block Design

The design of the Al-6061 reference block to study the diffraction of SV waves from a 90 degree corner of finite radius is shown in Figure 1. Ultrasonic pulses are launched and received by immersion probes, in order to avoid the variable coupling problems of contact probes; the probes may be located at any of the 6 locations shown in the Figure, plus one additional location used only for calibration/set-up. It is noted that losses due to beam spreading, attenuation in the metal and water, and mode conversion efficiency at the metal/water interface are identical for each of the six possible measurement locations of the transmitter and receiver; this allows the diffraction pattern to be measured as a function of angle without any corrections for variability in these parameters. A radius of 310 microns was machined into the 270-degree corner of the block; this value was selected to permit studies for values of ρ/λ ranging from 0.099 for 1 MHz probes, up to 1.981 for 20 MHz probes. The incident angle of the compression waves launched from the immersion probes towards the aluminum block is greater than the first critical angle, in order to minimize the presence of extraneous refracted compression waves inside the block.

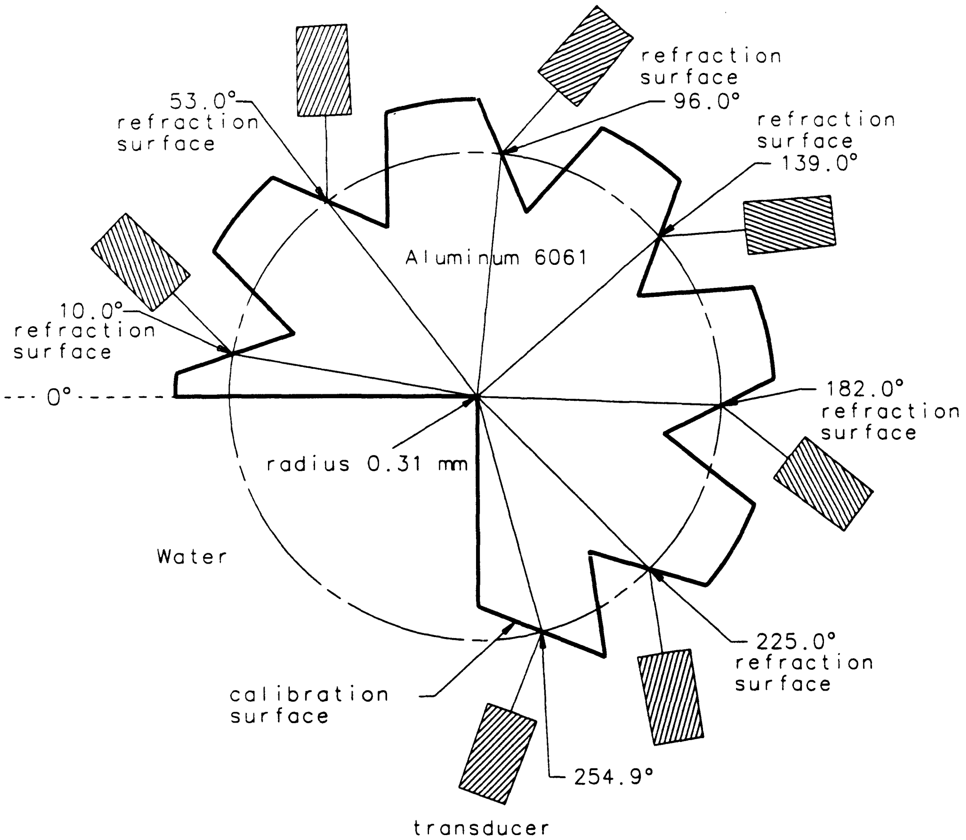

Figure 1. Aluminum reference block for measurement of diffraction pattern of vertically polarized shear waves impinging on a 270-degree corner of finite radius. Transmitter and receiver immersion probes can be place at any of 6 positions, in a pulse-echo or pitch-catch configuration. A calibration surface is provided for probe alignment and set-up.

Procedure

A matrix of tests was conducted using matched pairs of 1, 2, 5, 10, 12, 15, and 20 MHz transducers. At each frequency, the magnitude of the diffracted signal was measured for all possible combinations of 6 incident and diffraction angles. A pulse-echo technique was used for cases where the angle of incidence and angle of diffraction were the same; a pitch-catch technique was employed where the angles were different. To account for the vastly different strengths of transducers at various frequencies, all diffracted echo magnitudes were normalized by the strength of a signal obtained from the same probe(s) in a reference configuration. By this means, trends in the diffraction patterns as a function of ρ/λ can be studied in a single Figure for any given angle of incidence.

In an attempt to minimize the effects of noise or any imprecision in the machining of the block, all results were assembled in a B-Scan format, by collecting A-Scans along a 4-cm line parallel to the axis of the 270-degree corner. Only minimal variations in diffracted signal strength were noted in scanning along the axis of this reference block.

Results

Results of the diffraction amplitude measurements are shown in Figure 2; data are displayed as functions of incident angle, diffraction angle, and probe central frequency. Diffracted signals corresponding to the 15 MHz and 20 MHz probes proved to be too weak for analysis. Certain key features of the results are noted:

(a) For measurements taken at certain incident and diffraction angles, sound could travel directly from the transmitter to receiver probe without ever diffracting from the finite-radius corner. An example is shown in Figure 2(a) for a diffraction angle of 182 degrees; the large amplitudes noted at this nominal diffraction angle are not indicative of the efficiency at which sound was diffracted from the corner, and this data are therefore of little practical use.

(b) For measurements taken at certain incident and diffraction angles, ultrasound may be specularly reflected off the flat surface adjacent to the finite-radius corner, and travel on to the receiver probe. This leads to an exceptionally large signal, as seen for example at a nominal diffraction angle of 182 degrees in Figure 2(e); however, these data must also be discarded as they are not indicative of the way that sound interacts with the 270-degree corner.

(c) The general trend that large values of ρ/λ lead to specular reflection, while small values of ρ/λ lead to isotropic diffraction patterns, is evident in all the graphs of Figure 2. For example in Figure 2(c), diffraction data corresponding to the 1 MHz probe ($\lambda = 3.13$ mm, $\rho/\lambda = 0.099$) show a diffraction pattern that is somewhat more flat than those corresponding to the higher frequency probes, i.e., less angular dependence.

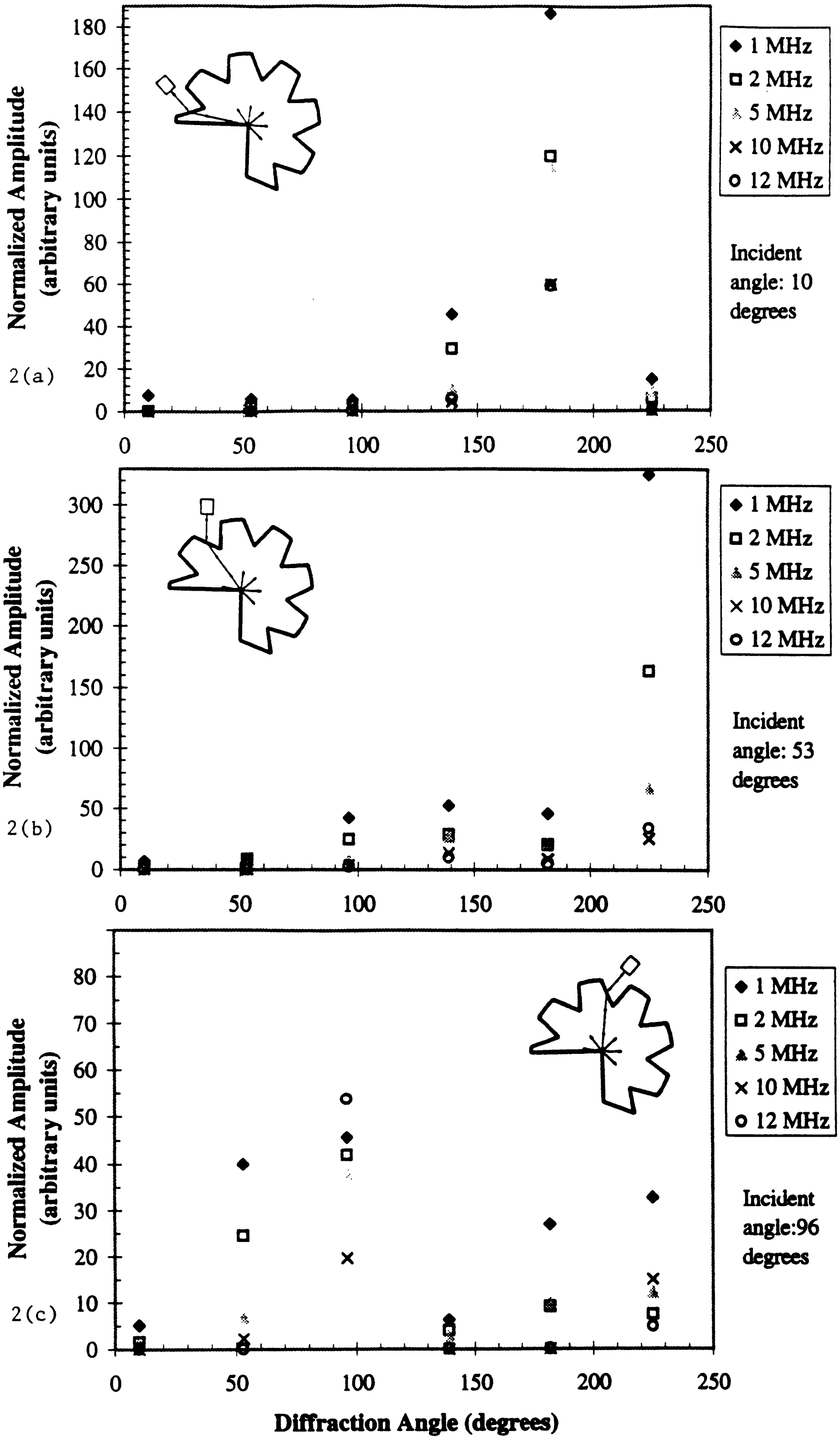

Figure 2. SV diffraction data from aluminum reference block.

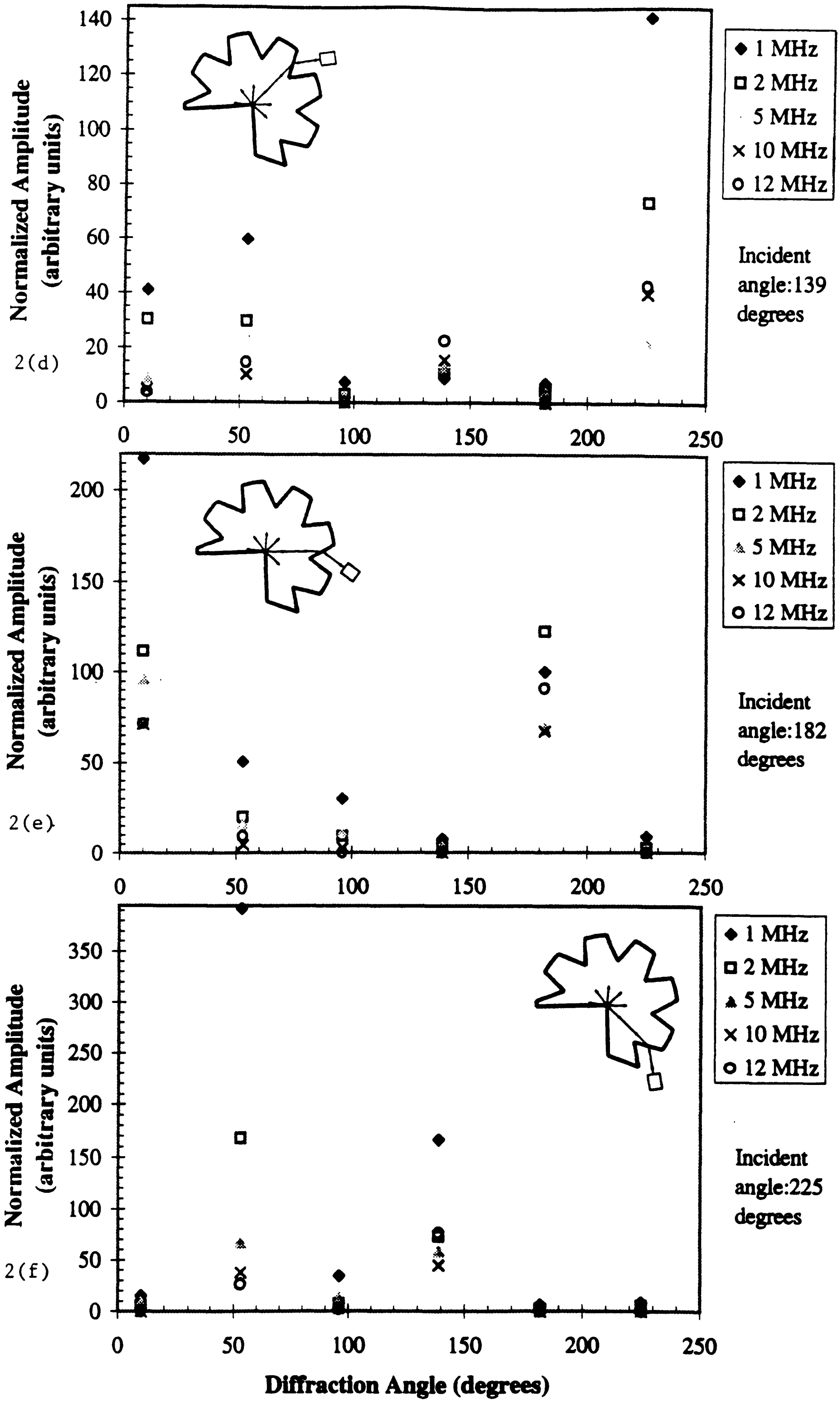

Figure 2 (continued). SV diffraction data from aluminum reference block.

The above observations lead to two possible procedures by which the radius of curvature at the corner of the block might be inferred from the diffraction pattern of ultrasound:

Method 1: Frequency Analysis

The corner is irradiated by a wide range of ultrasound frequencies (using multiple probes or a single wideband probe) at a single angle of incidence, and the diffracted wave amplitude is monitored as a function of frequency at a single angle. For very small values of ρ/λ (low frequency), the normalized diffracted wave amplitude will be relatively independent of frequency, and fairly small (isotropic scattering). At higher frequencies, the frequency dependence of the diffracted wave amplitude becomes stronger; the magnitude may actually shrink or grow depending whether specular reflection of sound towards the receiver probe is possible for the selected angles of transmitter and receiver. The normalized diffracted wave amplitude will again become independent of frequency in the high-frequency range corresponding to very large values of ρ/λ.

By monitoring the frequency range over which the above transitions occur, a rough estimate can be made of the frequency corresponding to $\rho/\lambda = 1$. Note that transmitter and receiver angles should be selected to avoid the problems noted in points (a) and (b) above, but rather angles for which the dependence of the diffracted signal magnitude on ρ/λ is most evident. For example, in Figure 2(c), the data at 53 degrees and 182 degrees indicate that we are in the diffraction "transition zone" at a frequency of about 2 to 5 MHz. This result would be more readily verified if data corresponding to a broader range of frequencies were available, but this presented experimental difficulties.

One obvious advantage to this technique is that it is relatively easy to implement: wideband transmitter and receiver probes can be permanently placed at fixed positions within an inspection fixture, and the data processed using Fourier analysis. A disadvantage, however, is that the critical frequency for which $\rho/\lambda = 1$ cannot be estimated very accurately. Preliminary results using this method to analyze simulated defects on a CANDU pressure tube wall confirmed the existence of the ultrasonic principles, but were not able to yield an accurate value for ρ ; details are given elsewhere [6].

Method 2: Directional Analysis

A second method to estimate ρ is to send low frequency narrow-band ultrasound pulses towards the corner from a fixed transmitter, and monitor the diffraction pattern as a function of angle. An isotropic diffraction pattern should result. The frequency is then slowly raised until a strong directional dependence becomes evident in the diffraction pattern, indicating that specular reflection has become predominant. The central frequency of this transition zone should roughly correspond to $\rho/\lambda = 1$.

An example of this technique is illustrated by Figure 2(d), at diffraction angles of dependence becomes evident, and becomes very prominent at 12 MHz.

An advantage of this technique over Method 1 is that the trend being monitored is much stronger and therefore easier to observe in an industrial setting. Method 2 would be relatively cumbersome to implement, however, as changes in the angle of the receiver probe would lead to shifts in water path lengths, attenuation, beam spreading, and refraction coefficients for sound travelling across the metal/water interface - these effects would all need to be taken into account when normalizing the received signals.

CONCLUSIONS

A novel test block has been developed that allows the diffraction pattern for vertically polarized shear waves incident on a 270-degree corner of finite radius to be measured as a function of incident and diffraction angles. SV diffraction patterns were collected for a range of ultrasound frequencies; general trends were consistent with those predicted by diffraction theory. Base on these results, two methods have been proposed by which ultrasonic diffraction principles can be used to estimate the root radius of curvature of a fretting wear defect in a CANDU pressure tube.

ACKNOWLEDGEMENTS

This work was supported by Ontario Hydro Technologies, the Canadian Natural Sciences and Engineering Research Council (NSERC), and the Ontario Ministry of Colleges and Universities URIF program.

REFERENCES

1. W. R. Fundamenski, "Inside Surface Defect Depth Measurement by Time of Flight Diffraction", Ontario Hydro Research Report No. 90-260-P (1991).
2. S.J. Davis and S.B. Palmer, Nondestructive Testing and Evaluation 5, 227 (1990).
3. M. deBilly *et al*, J. Appl. Phys. 61, 2140 (1987).
4. H. Zhu, L.J. Bond, and P.H. Albach, Ultrasonics 30, 301 (1992).
5. R.J. Blake and L.J. Bond, Ultrasonics 28, 214 (1990).
6. A.N. Sinclair *et al*, Proc 1993 IEEE Ultrasoinics Symposium, 745 (1994).